Published paper

Gonzalez-Valadez, M., Baltazar, A., Dwyer-Joyce, R.S. (2010) *Study of interfacial stiffness ratio of a rough surface in contact using a spring model*, Wear, 268 (3-4), pp. 373-379
http://dx.doi.org/10.1016/j.wear.2009.08.022

Study of Interfacial Stiffness Ratio of a Rough Surface in Contact Using a Spring Model

M. Gonzalez-Valadez [1,2], R.S. Dwyer-Joyce [2], A. Baltazar [3]

[1] CIATEQ, A.C., Av. Manantiales 23-A, Parque Industrial Bernardo Quintana, Querétaro, México. C.P. 76246.

Tel. number: +52 (442)1961500 Ext. 4225; *Fax number*: +52 (442) 1961500 Ext. 4231. *Email address*: miguel.gonzalez@ciateq.mx

[2] The University of Sheffield, Department of Mechanical Engineering, Mapping St., Sheffield, S1 3JD, UK.

[3] CINVESTAV- Unidad Saltillo, Robotics and Advanced Manufacturing Program, Carr. Saltillo-Monterrey km 13.5, Ramoz Arizpe, Coahuila, México.

Abstract

This study proposes the use of a simple spring model that relates the interfacial stiffness with the complex reflection coefficient of ultrasound in a rough contact. The spring model cannot be directly related to the real area of contact as this depends on the amount, shape and distribution of contacting asperities. However, it is clear that the model provides a non destructive tool to easily evaluate both longitudinal and shear interfacial stiffnesses and their ratio. Experimental findings indicate that the interfacial stiffness ratio K_τ/K_σ determined during loading/unloading cycles is sensitive to the roughness level and load hysteresis. The results deviate from the theoretical available micromechanical models, indicating that actual contacting phenomenon is more complex and other variables needed are not accounted for by the models.

Keywords: ultrasound, rough contact, interfacial stiffness

Introduction

The problem of mechanical contact of two elastic bodies has been of great interest to the scientific community. This has been mainly triggered by the need to predict contact area relevant in engineering to mechanical, electrical and heating conduction analysis. For two nonconforming surfaces the properties of the interface depends on the random contact of the surfaces. In a contact between rough surfaces only very few asperities go into contact. Therefore, high local stresses take place at the individual asperity tips causing an immediate plastic deformation and forming cold-welded junctions between the metal surfaces. Additionally, with the application of normal loading-unloading cycles, hysteresis phenomenon due to elastic and plastic deformation has been reported in the literature (i.e. [1], [2], [3]).

The development of experimental tools to investigate rough contact has been a slow ongoing process. Methods based on electrical and thermal conduction, measurement of fluid flow through the contact and the neutron-graphic method are useful to calculate real contact area but cannot provide an estimation of interfacial stiffness [4]. Kendall & Tabor [5] have found different drawbacks with the methods based on electrical and thermal conduction as well as with optical methods when used in real engineering contacts. When two nominally flat specimens are pressed together by normal force, the deformation of asperities can be recorded by means of an electric micrometer or by the stylus of a profilometer. However, in practical applications, the results need to be refined by eliminating the effect of surface deformation in the test machine. Krolikowski & Szczepek [4] indicated that using the method based on direct measurements of compliance, the measurable limit of interfacial stiffness of a rough contact is about 1 GPa μm^{-1}.

From the original independent investigations carried out by Kendall & Tabor [5] and Tattersal [6], it was clear that the reflection coefficient of ultrasound can be related to the interfacial stiffness of a rough contact by means of a spring model; however, it is not directly related to the actual contact area as it was hypothesized in their study. Therefore, the results show serious disadvantages of the method, but it can be a powerful tool when the stiffness is the main parameter to assess. In fact, in this paper the ratio of tangential to normal stiffness is evaluated utilizing the spring model of Kendall & Tabor [5].

Several theoretical approaches have been developed that can be applied to the contact between two nominally flat surfaces, one smooth undeformable against a rough deformable with isotropic statistical properties of roughness [7, 8, 9, 10]. Although the models work for idealized shape of asperities and non-interacting assumption, an estimation of the real area of contact and nominal pressure can be obtained.

Studies on normal stiffness have been reported more often than on shear interfacial stiffness. However, the use of both normal and shear stiffness expressed as a ratio can be used to determine the nature of contact [11]. The shear stiffness can be obtained from a pre-stressed condition in which a normal load to the interface is followed by a small shear force. This is a special case which requires only the application of a small elastic dynamic shear load (pre-stressed interface). Ultrasonic shear waves applied in this way deform the interface only elastically because of the small-scale loading-unloading cycle, centered on the static stress [3]. Therefore, no additional plastic deformation at the asperities occurs independently of the state of the deformation of asperities produced by the normal load. Berthoud and Baumberger [12] reported direct measurements of shear stiffness versus displacement on a pre-stressed rough interface. The experiments have provided evidence that indicates that a multi-contact interface subjected to the small shear deformations has an elastic response. Ultrasonic studies of shear stiffness versus load can be found in several publications [4, 13, 14, 16].

The ratio of interfacial stiffness ratios has been anticipated as an important parameter to characterize an imperfect interface. Nagy [11] presented a comprehensive review to show how this can potentially be used to distinguish perfect contact from kissing, slip, or partial contact. For rough surfaces, the possibility of distinguishing welded condition has been of interest. Recently, several works on the interfacial stiffness ratio from a rough interface have been published [12, 15, 16] where loading and unloading cycles on the interface were applied.

The analysis carried out by Krolikowski & Szczepek [16] which combines the contact model of Greenwood & Williamson [8] with the equation of Johnson [17] for small tangential displacement, revealed that the ratio of tangential to longitudinal stiffness is solely dependent on the Poisson ratio of the contacting rough surfaces. Similarly, by using the equation of Hisakado & Tsukizoe [18] for small tangential displacements of contacting asperities, Sherif & Kossa [15] also concluded that the ratio of stiffnesses can be calculated only from the Poisson ratio of both surfaces in contact.

Recently, Baltazar et al. [14] described a theoretical model, similar to the previously obtained by Krolikowski & Szczepek [16] and Mindlin [19], but which includes a correction factor accounting for the angle of misalignment. Predictions of the model are very close to those made through the Sherif & Kossa approach [15]. Additionally, a slight increase in the ratio of stiffnesses observed on increasing nominal pressure was attributed to misalignment at a single asperity contact. The model is again non dependent on the distribution of contact asperities.

Yoshioka & Sholtz [20] provide a comprehensive model of elastic contact that allows for the oblique contact in both the normal and shear directions. Nagy [11] worked with the original approach of the model of Yoshioka & Sholtz [20] for a chi squared distribution of asperities. It was found that the ratio of tangential to longitudinal stiffness is exclusively dependent on the Poisson ratio of the contacting materials.

This work has three objectives: first, to develop a phenomenological understanding of the correlation between interfacial stiffness ultrasonically determined and the state of deformation of a rough surface; second, to determine interfacial stiffness ratio K_τ/K_σ for different roughness levels; and third, to investigate the hysteretic behavior of K_τ/K_σ and its relationship to the deformation of asperities at the interfaces.

Micromechanical Description

Krolikowsky and Szczepec [16] provide a mathematical formulation that incorporates the Hertz-Mindilin theory [19] and the contact model of Greenwood and Williamson [8]. The method models the complex contact between rough surfaces as a normally distributed set of elastic spheres contacting against an elastic plane of the same material loaded with a normal force f and a tangential force s [19, 21, 22]. Both mean contact pressure P, and mean tangential stress τ, are as follow

$$P = D_s \frac{2E}{3(1-v^2)} R^{1/2} \sigma^{3/2} \int_t^\infty (x-t)^{3/2} \phi(x)\, dx, \tag{1}$$

$$\tau = sD_s \frac{2E}{(2-v)(1+v)} R^{1/2} \sigma^{1/2} \int_t^\infty (x-t)^{1/2} \phi(x)\, dx, \tag{2}$$

where D_s is the summit density per unit area, R is the radius of curvature of the elastic sphere, E is Young's modulus, v is the Poisson's ratio, σ is the variance of summit height distribution, x is the normalised height of summits, t is the normalised separation and $\phi(x)$ is the normalised height distribution function of the summits.

Thus, the normal K_σ and tangential K_τ stiffness per unit area for this model are

$$K_\sigma = -\frac{1}{\sigma}\frac{dP}{dt} = D_s \frac{E}{1-\nu^2} R^{1/2}\sigma^{1/2}\int_t^\infty (x-t)^{1/2}\phi(x)dx\,, \qquad (3)$$

$$K_\tau = \frac{d\tau}{ds} = D_s \frac{2E}{(2-\nu)(1+\nu)} R^{1/2}\sigma^{1/2}\int_t^\infty (x-t)^{1/2}\phi(x)dx\,. \qquad (4)$$

Combining Equations (3) and (4) yields the tangential to the normal contact stiffness ratio

$$\frac{K_\tau}{K_\sigma} = \frac{A(1-\nu)}{(2-\nu)}, \qquad (5)$$

with A=2, which is also identical with that for the elementary contact previously formulated by Mindlin [19] and more recently by Johnson [7] for two spherical bodies in contact. The form of equation (5) has been corroborated in several studies which differ basically in the values of the coefficient A. For instance Sherif & Kossa [15] found a theoretical value for $A = \pi / 2$. For the model of Yoshioka & Sholtz [20], Nagy [11] obtained an approximated value for $A \approx 0.71$. In the model presented by Baltazar et al. [14], A has a changing value expressed as

$$A = \frac{2\xi}{\psi}, \qquad (6)$$

where ξ and ψ are correction factors accounting for the geometrical misalignments in respect to shear and longitudinal directions, respectively [23]. The factor ψ takes values of about 1 for angles below 50° assuming non-slip condition at the asperities. The factor ξ typically was found to vary between 0.6 and 0.8.

Ultrasonic Response of a Rough Surface Contact

Figure 1a schematically shows the reflection of a sound wave from a rough surface interface. At the contact region sound waves would pass through while at an air gap it would be totally reflected. The proportion of the amplitude of an incident wave that is reflected is known as the reflection coefficient, *R*. Conversely, the amplitude of the incident wave transmitted trough the contact spots is the transmission coefficient, *T* (see figure 1).

Thus for two like materials, the reflection coefficient varies from $R=0$ for complete contact to $R=1$ for no contact (i.e. a solid air interface). If the nominal pressure across the interface is increased, asperity tip deformations cause both the interface to close slightly and the real area of contact to increase. Kendall and Tabor [5] showed that when the wavelength of the ultrasonic wave is large compared with the size of the asperity contacts, the reflection is a function of the interface stiffness, *K*. As a consequence of the simple quasi-static spring model, the reflection coefficient can be found as (shown schematically in figures 1b and 1c)

$$R = \frac{1}{\sqrt{1+\left(\frac{2K}{\omega z}\right)^2}}, \qquad (7)$$

where z is the acoustic impedance of the material on either side of the interface and ω is the angular frequency of the ultrasonic wave. This relationship holds for both longitudinal and shear wave reflections (the longitudinal and shear wave speeds are used, respectively). A similar expression exists for two dissimilar materials pressed together [24]. This model has been used extensively to study the reflection and transmission of sound across incomplete interfaces [2, 4, 11, 13].

Drinkwater et al. [25] demonstrated that the stiffness of a range of contacts of varying roughness is well represented by equation (7). They studied the reflection as a function of the frequency of the ultrasonic wave. The reflection coefficient was found to be dependent on frequency, but the predicted stiffness was shown to be independent of frequency.

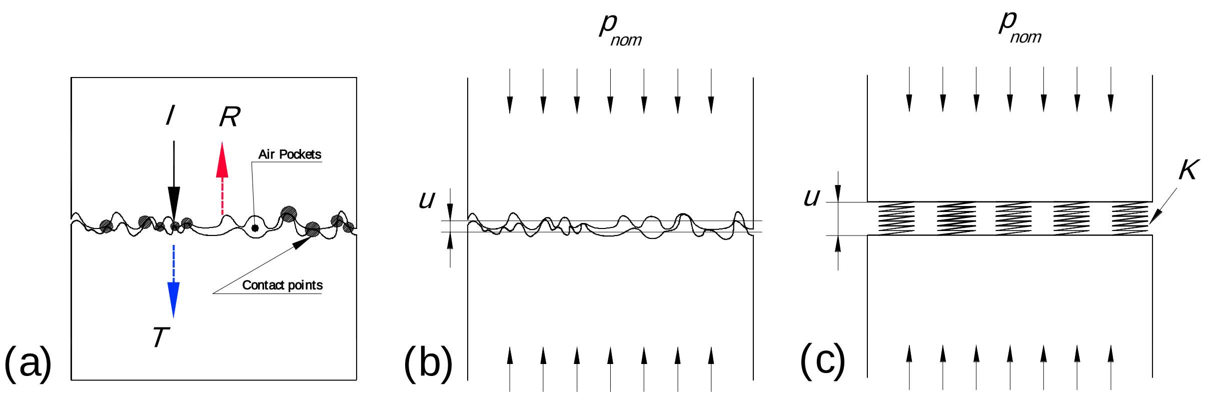

Figure 1. Scheme showing a representation of the ultrasonic response of rough surface contact, a) reflection, b) loading and deflection, and c) the spring model representation.

Experimental Set-up

Figure 2 shows the loading frame and the arrangement of the ultrasonic equipment used in the tests. Two ultrasonic pulser-receivers were arranged to make it possible for the longitudinal and shear signals to simultaneously be processed. The specimens were subjected to loading-unloading cycles of compressive pressure in a hydraulic frame operating in load control mode. The upper specimen had a disk of piezoelectric material glued to the back face with a temperature stable contact adhesive. The transducer was of the wrap around electrode type so both wires could be soldered directly to the top face of the ≈5MHz shear wave transducer. The lower specimen was interrogated by means of a 5MHz longitudinal wave planar contact transducer. The upper specimen was loaded against the lower specimen, through an annulus with a hemispherical cap. The hemispherical end piece allowed the upper specimen to align against the lower in order to obtain a more distributed and conformed contact.

The contacting interfaces were made from steel specimens. The contacting face of the bottom specimens were ground and polished, while those of the upper specimens were grit-blasted (see Figure 3). All surfaces were measured using a surface profilometer before and after the loading experiments (Table 1).

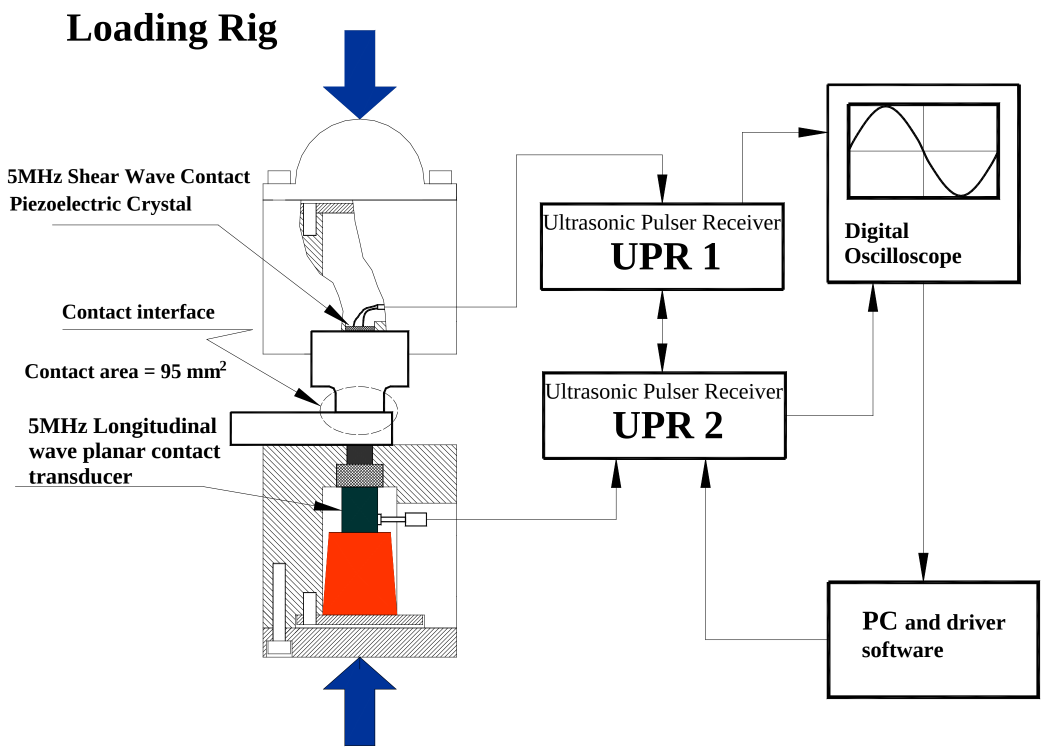

Figure 2. Schematic diagram showing loading rig, specimens and ultrasonic measuring apparatus.

Two ultrasonic pulser-receivers (UPR) were used to generate simultaneously voltage pulses to actuate the transducers. Both shear and longitudinal transducers had a central frequency of 5 MHz. The reflected pulses were received by the digital oscilloscope, amplified, and passed to the PC for signal processing.

Before both specimens are pressed together, a reference signal of ultrasound is taken. This signal is taken at the point where no contact exists. In these cases the entire incident waves, shear and longitudinal, at the interface are reflected completely (and virtually none is transmitted at the metal-air interface). The assumption that the incident wave fully reflects in an interface of solid-air, is backed by the fact that air poses very low acoustic impedance (400 Ns/m^3), as opposed to steel ($47x10^6$ Ns/m^3). This is the reason why air is considered a pure reflector or mirror to ultrasound. These signals are therefore equivalent to the incident signals, and are used as reference pulses

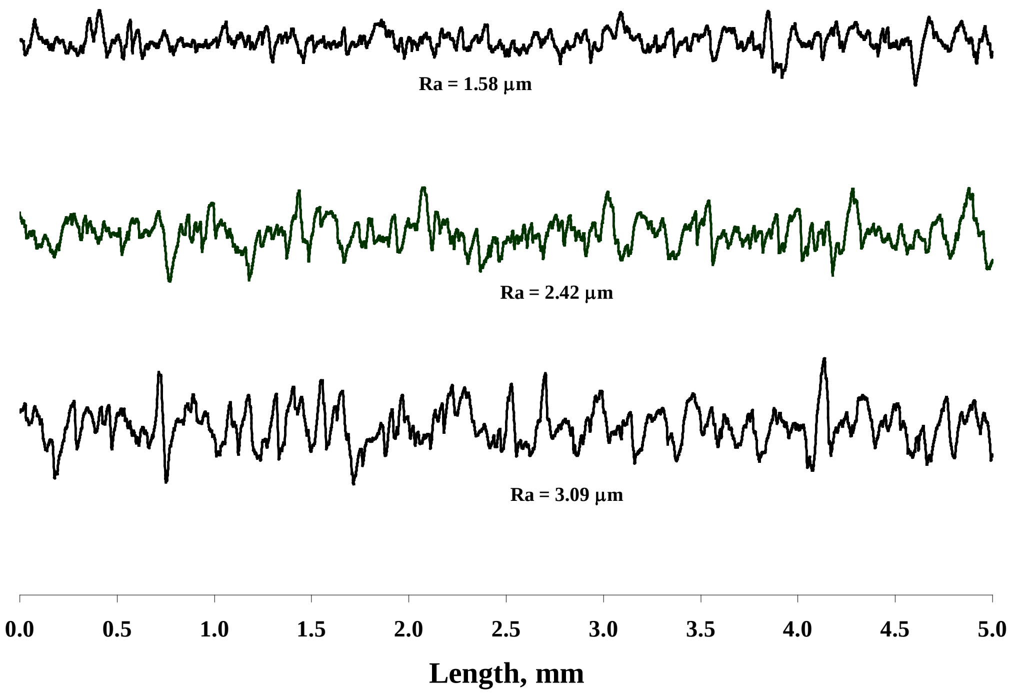

Figure 3.Different grit blasted upper specimens used in the experiment.

Material	R_a in upper specimens		R_a in bottom specimens	
	Before Loading	After Loading	Before Loading	After Loading
Grit-blasted steel 1	1.58	1.18	0.03	0.07
Grit-blasted steel 2	2.42	1.52	0.04	0.16
Grit-blasted steel 3	3.09	1.82	0.04	0.13

Table 1. Roughness before and after test (sample length 5 mm, each result is an average of three profiles). Both specimens are made up of steel.

The test specimens are then loaded together and subsequent reflected pulses are recorded. The load is applied gradually by steps until reaching a maximum nominal pressure of 400MPa. The loading steps consist basically of applying the load from zero to the maximum with a tension-compression machine. In the same way, the unloading process is executed by decreasing the load from the maximum value to 5MPa. It should be ensured that the contact interface not be downloaded completely as this would involve a different set of asperities to come into contact in the next loading-unloading cycle.

A Fourier transform is performed on both the reflected and reference signals; dividing one by the other gives the reflection coefficient spectrum. For a rough surface interface this reflection coefficient depends on the frequency. Equation for the reflection coefficient (Equation (7)) is then used to obtain the interfacial stiffness which should be independent of frequency. In practice, there is little statistical variation due to noise in the signal, and a mean stiffness is determined for all frequencies within the transducer´s bandwidth. More details of this method for determining interface stiffness ultrasonically can be found in Dwyer-Joyce et al. [2].

Results

Figures 4, 5 and 6 show the experimental results of interfacial stiffness versus normal pressure. Both interfacial stiffnesses, shear and longitudinal, were calculated with equation (7). Acoustical impedance z, for shear and longitudinal waves were calculated uisng typical values of speed of sound for steel: 5900 m/s and 3100 m/s, respectively [26]. It can be observed that the normal stiffness during the loading step of the first cycle in terms of normal pressure follows an approximate linear relationship [27, 28]. This behaviour has previously provided a simple calibration route for maps of contact stiffness and other studies [29]. It is clear that to predict the normal pressure from stiffness measurement in a contacting joint, their roughness has to be reproduced in laboratory specimens and the predictions would only be useful for the first loading.

The curve of the unloading process in all cases follows a different path than that of the loading step, showing a hysteresis phenomenon. This also indicates that most of the asperity plasticity has been achieved at this stage. It has been previously recognized that the first loading on the contact interface always surpasses the elasticity of asperities and therefore occurs in elasto-plastic conditions [3]. The ultrasound is not strongly affected by the plasticity of the contact, and it depends basically on the increase of contact area with load.

After the first loading-unloading cycle, and to ensure that remaining plasticity is fully removed and the contact is occurring in elastic conditions, 10 more complete cycles were applied. Under these conditions, the normal and shear deformations are caused by the passage of a very small displacement wave, which causes only elastic deformation. The results also show that there is a small increase in interfacial stiffness possibly due to plastic deformation being added at the end of each loading cycle. The reason for this phenomenon is not fully understood. However, in a recent study, Gonzalez & Dwyer-Joyce [30] found that two things can be producing such an effect: stress relaxation and creep which happens when a stress is sustained for a period of time.

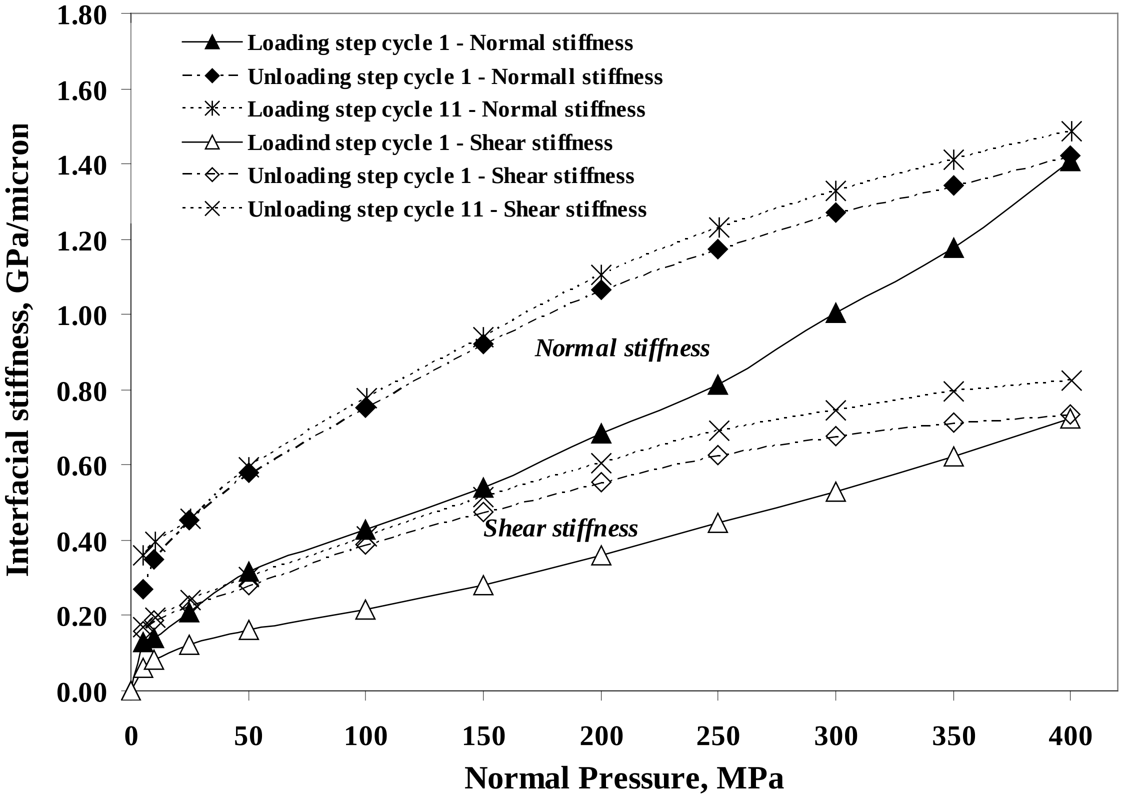

Figure 4. Normal pressure vs. interfacial stiffness for a steel-steel interface. The upper specimen had a roughness value Ra=1.58 μm before test.

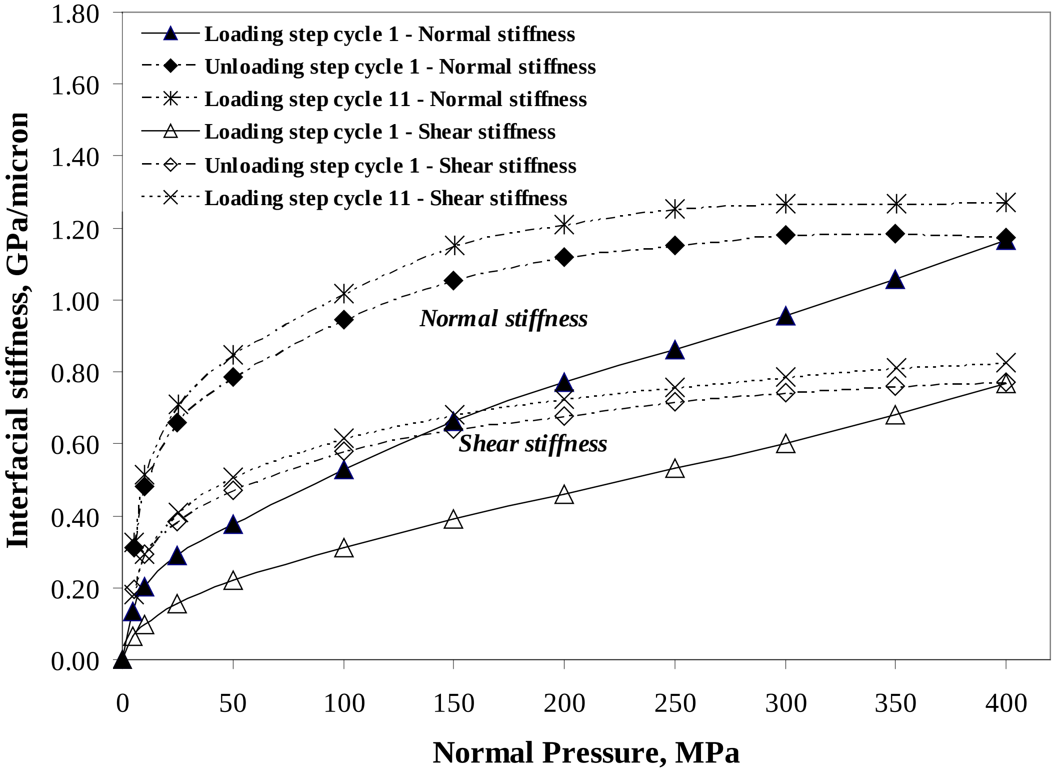

Figure 5. Normal pressure vs. interfacial stiffness for a steel-steel interface. The upper specimen had a roughness value Ra=2.42 μm before test.

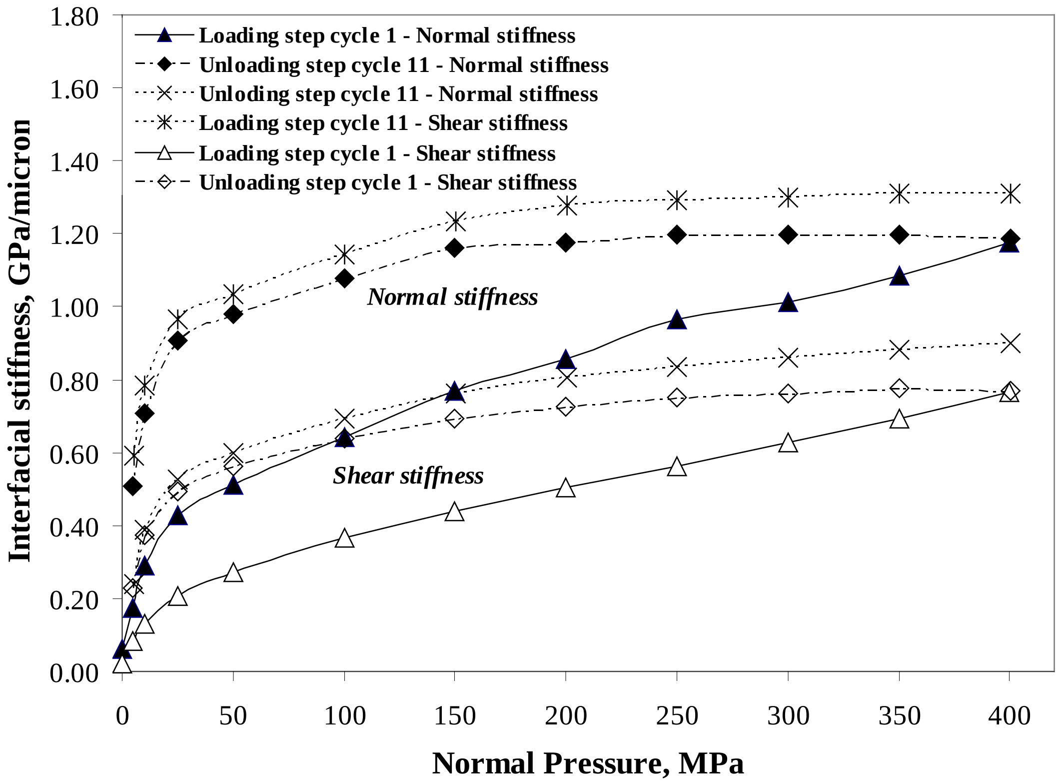

Figure 6. Normal pressure vs. interfacial stiffness for a steel-steel interface. The upper specimen had a roughness value, Ra=3.09 μm before test.

To simplify the plots, in figures 4, 5 and 6 only the curves of the loading step of cycle 11 are shown. It is important to notice that one could use either the loading curve or unloading curve as the values are basically the same. The values of stiffness are higher for the contact interface with the least roughness. In the three different samples, the shear stiffness produces similar curves to those of normal stiffness.

Analysis and Discussion

Figures 7- 9 show plots of longitudinal stiffness ratio as function of normal pressure. In addition, the theoretical predictions found in previous literature are compared to the experimental results (Figure 10). Data from the 1^{st} and 11^{th} loading-unloading cycles were used for comparison. This makes it possible to see what happens in an elasto-plastic contact (first loading-unloading cycle) and in a pure elastic contact (eleventh loading-unloading cycle). Equation (5) with a Poisson ratio ν=0.3 was used to estimate the theoretical predictions. Our experimental results show a dependence of K_τ/K_σ ratio on load and *rms* roughness. For higher values of roughness, K_τ/K_σ has a larger mean value. Also, it can be seen that for high values of roughness there is an increment in the variation rate of K_τ/K_σ. Clear hysteresis is observed for mild and high *rms* roughness (Figures 7 and 8), and almost none detected for smooth surface. In the last case, a region of constant load independent ratio is observed. The results indicate an apparent sensibility to plastic deformation during the first cycles and almost none existent for additional loading cycles.

In the cases studied, the results deviate from the theoretical values predicted by Mindlin [19]. It can be seen that only for high pressure (Figures 8 and 9) the values approach theoretical ones in Eq. (5) with A=2. It is interesting to note that the lower ratio values are always found for the first loading.

The results for smooth surface shows some agreement with theoretical predictions of Sherif & Kossa [15] and Baltazar et al. [14]; this last is estimated assuming an average value of the correction factor ξ=0.7. Only for this case, it can be suggested that the stiffness ratio is solely dependent on Poisson´s ratio, and virtually constant for both elasto-plastic contact and pure elastic. The reason for the behavior which in principle could indicate a fixed relationship (i.e. load independent ratio) between normal and shear stiffness at some pressure value needs further investigation. Even though some theories agree with experimental results, it is also observed that the equation in Krolikowski & Szczepek [16] over predicts the experimental findings of our study ((K_τ/K_σ=0.82). In contrast, the model of Yoshioka & Scholz [20] predicts values significantly lower than experimental data ($K_\tau/K_\sigma\approx$0.29) (see Fig. 10).

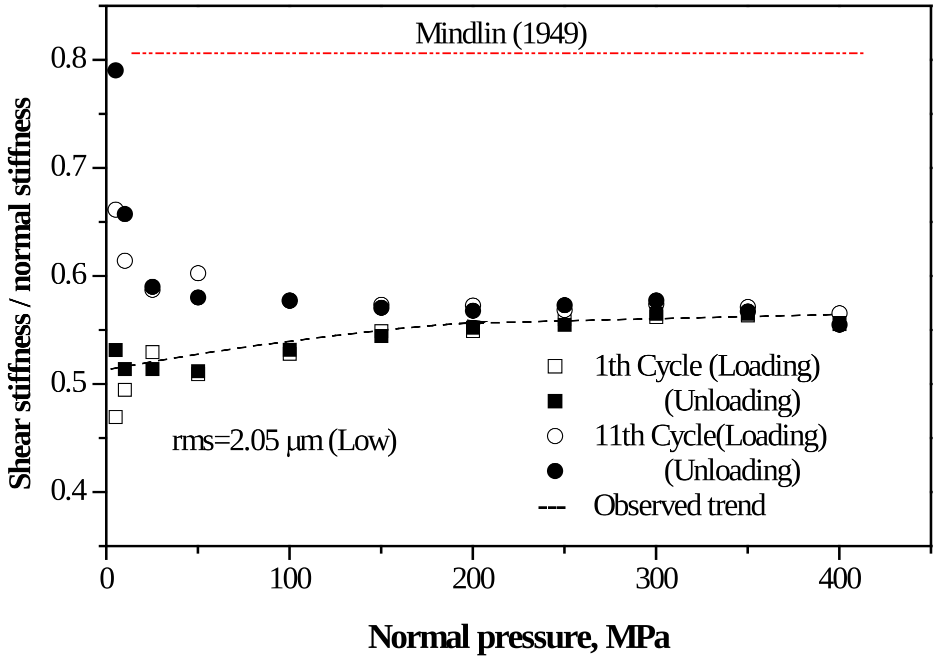

Figure 7. Experimental results of interfacial stiffness ratio as function of loading cycles for smooth sample 1 (Ra=1.58 μm). Points indicate experimental data and the dashed line is the observed trend.

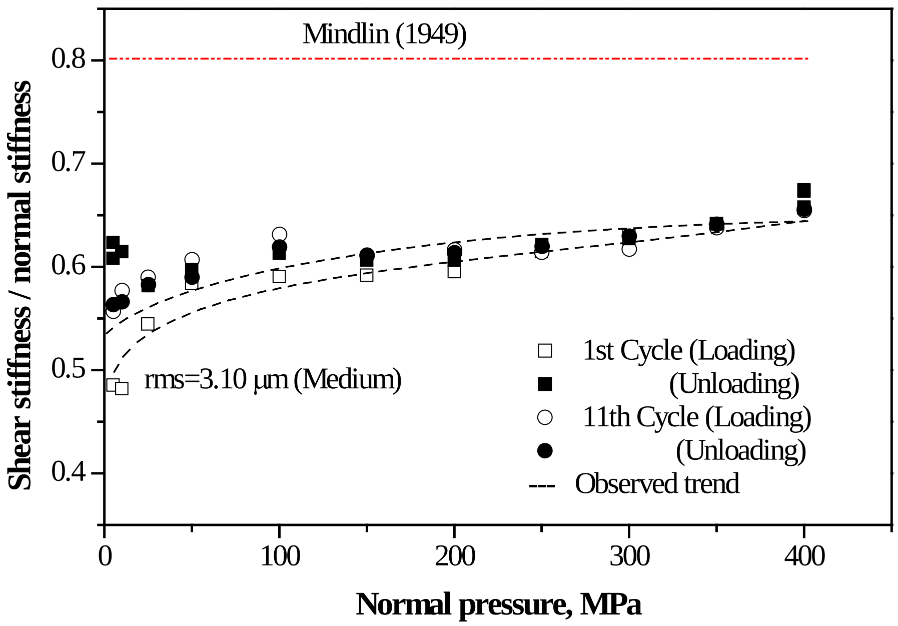

Figure 8. Experimental results of K_τ/K_σ versus normal pressure for rough sample 2 (Ra=2.42 μm).

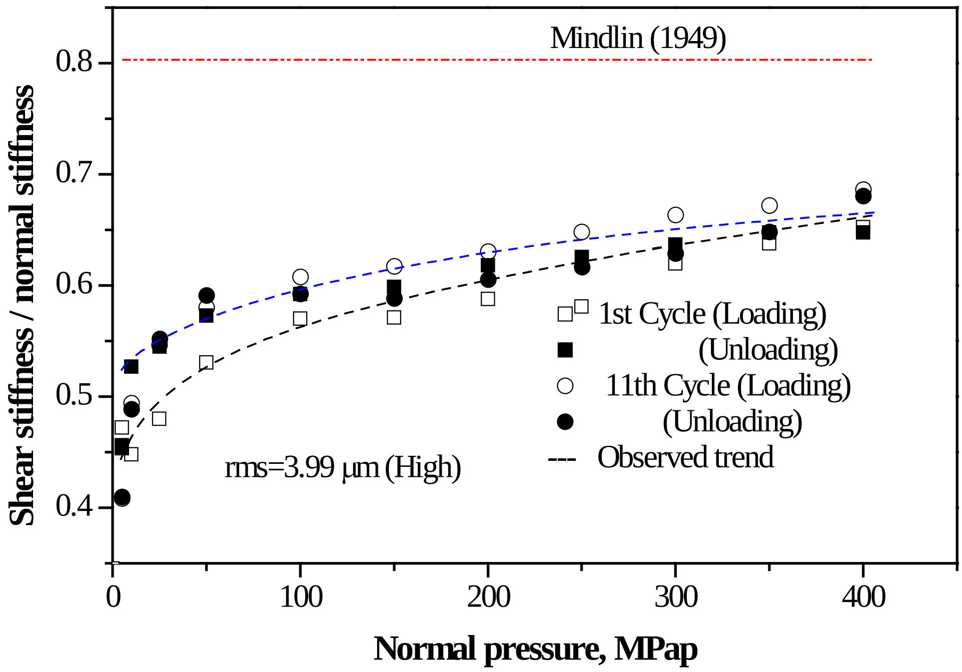

Figure 9. Experimental results of K_τ/K_σ versus normal pressure for rough sample 3 (Ra=3.09 μm).

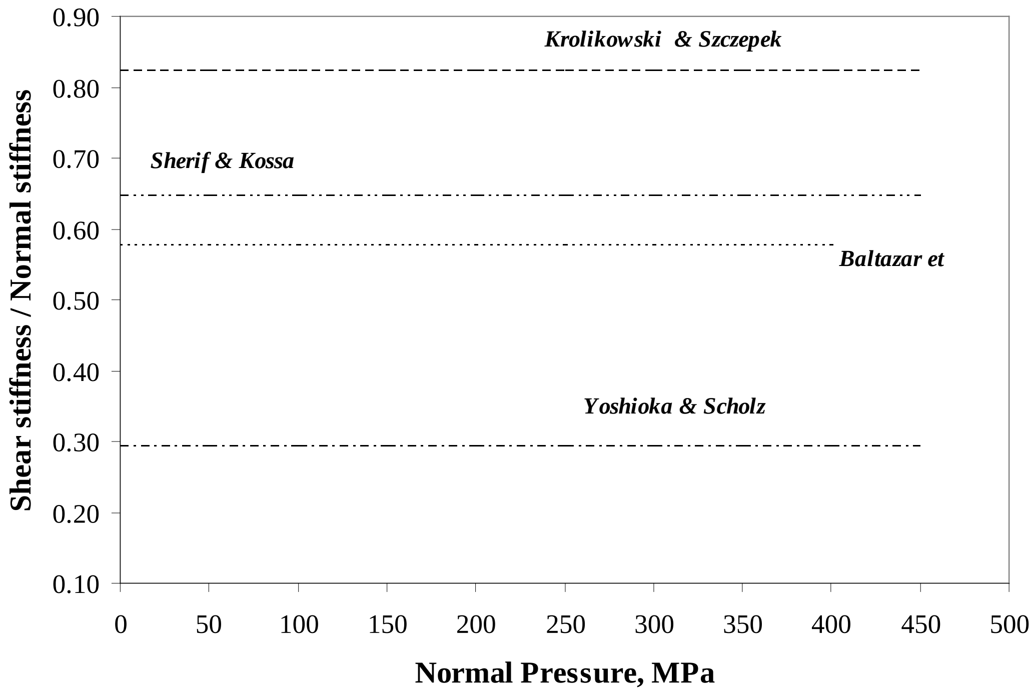

Figure 10. Theoretical predictions of shear to normal stiffness ratio.

On the other hand, ultrasonic waves are sensitive to the surface roughness but only for high frequencies when the wavelength is comparable with the height *h* of the interface. When this condition is not reached, QSA model can be used to describe the deformation of the interface Yalda-Mooshabad et al. [31]. In our case, the wavelength in steel for longitudinal wave and a frequency of 5MHz is about 1.18 mm. This value is much larger than the *rms* roughness of the interface.

From our experimental results, it is possible that an additional mechanism of wave interaction with the interface can be observed by measuring the stiffness ratio as function of pressure. In principle, two conditions could be affecting the ultrasonic reflection signature, the contact at the roughness asperities and the space (voids) left in between the asperities. It is clear that by bringing the rough surface together, the aspect ratio will change up to a point where the valleys get flatter. This condition is not accounted by the micromechanical model since it is built under the assumption of independent asperities deformation. Since the observed variation of aspect ratio during loading is controlled by the contact area, it is possible that the effect of voids is masked by the contact behavior and it is only unveiled when the ratio K_τ/K_σ versus pressure is estimated.

A review of the effect of non-interacting voids on the ultrasonic signature was given by Nagy [11]. According to the study, the interfacial stiffness ratio was found to be sensitive to the aspect ratio $\xi = a / b$ of spheroidal voids, where a is the out-of-plane and b the in-plane dimension. It was shown that the ratio K_τ/K_σ of two similar solids (v=0.3) in contact varies monotonically from 0.45 for spherical void ($\xi \to 1$) to 0.88 for flat cracks ($\xi \to 0$). Following a different approach, calculations of interfacial ratio using boundary element method (BEM) and Independent Scattering Approach (ISA) were estimated by Yalda-Mooshbad et al. [31]. In their calculation for an interface with a fraction area of voids of 2.5% in a matrix with properties c_l =6.0 Km/sec and c_t=3.0 Km/sec, the ratio was found to vary monotonically from 0.36 for spherical void ($\xi = 1$) to 0.76 for flat cracks ($\xi = 0.05$).

To estimate the mean aspect ratio in our tested surface, an approximation based on the statistical parameters of the samples (Table 2) was carried out following the analysis of Nayak [33]. It was found that the determined mean aspect ratio in the fresh surfaces does not change considerably for samples 2 and 3, with only a decrement of about 25% for the smoothest sample (Ra=1.58μm). These values of aspect ratio give a K_τ/K_σ of about 0.78 from Nagy [11] and about 0.76 from Yalda-Mooshbad et al. [31]. The values are higher than our experimental findings, but it should be noted that the statistical results of samples 2 and 3 show a positive correlation between experimental K_τ/K_σ and estimated aspect ratio. However, the smooth sample 1 has a lower than expected value of K_τ/K_σ as one would predict based on its aspect ratio.

Another relevant parameter for our study is the mean curvature which is shown experimentally to vary proportional to roughness (Table 2); higher asperities are expected to have larger mean curvature [32]. For fresh surfaces, the aspect ratio is a random variable, which could be correlated with the distribution of asperities and curvatures [33]. If we relate the values of curvature with the misalignment of contact proposed by Baltazar et al. [14], the correction factor would be between 0.9-0.8 resulting in a K_τ/K_σ value of about 0.65 for samples 2 and 3 and a bit larger for sample 1 with a smooth surface. The result for the smooth surface is in the opposite direction to the expected direction of correlation between interfacial ratio and the mean curvature.

Sample	σ_{rms}	m_o (μm^2)	m_2	m_4 (μm^{-2})	α	k_m *(Degree)*	d_{sum} (μm)	***Aspect ratio***
1 Ra=1.58 μm	2.04	4.22	0.046	0.011	24.70	24.30	130.50	0.031
2 Ra=2.42 μm	3.10	9.70	0.074	0.015	27.50	30.50	154.10	0.040
3 Ra=3.09 μm	3.90	15.28	0.100	0.018	27.70	32.70	175.00	0.044

Table 2. Additional experimental statistical parameters for the samples studied. σ_{rms} is the *rms* roughness, m_0, m_2, m_4 are the spectral moments of the surface, α is a parameter related with the width of spectrum, k_m is the mean curvature, and d_{sum} is the mean distance between summits.

From the above discussion, there is no clear evidence to indicate if any of the two proposed parameters: radius of curvature or aspect ratio is solely controlling the observed stiffness ratio variation during the loading cycles.

It is also possible that if the stiffness ratio is truly constant at the asperities contact, then the ratio variations are related to change in the shape of the voids. However, the shape of the voids is controlled by the contact of asperities. Therefore, any change in the contact area at the asperities will control the variations of the voids. This empirical analysis could explain the observed hysteresis, which is expected for large plastic deformation and correlated with the larger roughness.

The problem is far from being resolved, and the experimental results show that the micromechanics of shear contact may be more complex than expected, with that said, mechanics such as slip and/or ellipsoidal contact just to mention a few, could be affecting the interfacial ratio [34, 35].

Conclusions

An ultrasonic approach has been used to determine the normal and shear stiffness for three different grit-blasted contacting surfaces. Experimental data of stiffness ratio was found to be sensitive to both roughness level and plastic deformation. Degree of hysteresis for the loading/unloading cycles was found to be a function of the roughness level. The assumption of ultrasonic wave sensitivity to other roughness parameters such as aspect ratio of voids and radius of curvature did not completely follow our experimental findings. A non-constant stiffness ratio suggests that additional parameters other than those that describe the Hertzian contact are being unveiled by the interfacial stiffness ratio.

References

1. D. Tabor, The Hardness of Metals, Oxford University Press, USA, 2000, p.192.
2. R.S. Dwyer-Joyce, B.W. Drinkwater, A.M. Quinn, The use of ultrasound in the investigation of rough surface interfaces, ASME Journal of Tribology 123 (2001) 8-16.
3. J.Y. Kim, A. Baltazar, S.I. Rokhlin, Ultrasonic assessment of rough surface contact between solids from elastoplastic loading-unloading hysteresis cycle, Journal of the Mechanics and Physics of Solids 52 (2004) 1911-1934.
4. J. Krolikowski, J. Szczepek, Prediction of contact parameters using ultrasonic method, Wear 148 (1991) 181-195.
5. K. Kendall, D. Tabor, An ultrasonic study of the area of contact between stationary and sliding surfaces, Proceedings of the Royal Society of London: Series A 323 (1971) 321-340.
6. H.G. Tattersall, The ultrasonic pulse-echo technique as applied to adhesion testing, Journal of Applied Physics: Part D 6 (1973) 819-832.
7. A.W. Bush, R.D. Gibson, T.R. Thomas, The elastic contact of a rough surface, Wear 35 (1975) 87-113.
8. J.A. Greenwood, J.B.P. Williamson, 1966. Contact of nominally flat surfaces, Proceedings of the Royal Society of London: Series A 295 (1966) 300-319.

9. D.J. Whitehouse, J.F. Archard, The properties of random surfaces of significance in their contact, Proceedings of the Royal Society of London: Series A 316 (1970) 97-121.

10. R.A. Onions, J.F. Archard, The contact of surfaces having a random structure, Journal of physics, D: Applied Physics 6 (1973), 289-304.

11. P.B. Nagy, Ultrasonic classification of imperfect interfaces, Journal of Nondestructive Evaluation 11 (1992) 127-139.

12. P. Berthoud, T. Baumberger, Shear stiffness of a solid-solid multicontact interfase, Proceedings of the Royal Society: Series A 454(1998) 1615-1634.

13. R. S. Dwyer-Joyce, B. W. Drinkwater, A. M. Quinn, The Use of Ultrasound in the Investigation of Rough Surface Interfaces, Journal of Tribology, 123 (2001) 8-17.

14. A.Baltazar, S.I. Rokhlin, C. Pecorari, On the relationship between ultrasonic and micromechanical properties of contacting rough surfaces. Journal of the Mechanics and Physics of Solids 50, (2002) 1397-1416.

15. H.A. Sherif, S.S. Kossa, Relationship between normal and tangential contact stiffness of nominally flat surfaces, Wear 151 (1991) 49-62.

16. J. Krolikowski, J. Szczepek, Assessment of tangential and normal stiffness of contact between rough surfaces using ultrasonic method, Wear 160 (1993) 253-258.

17. K.L. Johnson, Contact Mechanics, Cambridge University Pres, New York, 1987, p.464.

18. T. Hisakado, T. Tsukizoe, Effects of distribution of surface slopes and flow pressures of contact asperities on contact between solid surfaces, Wear 30 (1974) 213-227.

19. R.D. Mindlin, Compliance of elastic bodies in contact, Journal of Applied Mechanics 71 (1949) 259-268.

20. N. Yoshioka, C.H. Scholz, Elastic properties of contacting surfaces under normal and shear loads: Part 1 – Theory, Journal of Geophysics Research 94 (1989) 17681-17690.

21. J.J. O´Connor, K.L. Johnson, The role of surface asperities in transmitting tangential forces between metals, Wear 6 (1963) 118-139.

22. M. Raoof, R.E. Hobbs, Tangential compliance of rough elastic bodies in contact, ASME Journal of Tribology 111 (1989) 726-729

23. K.Yamada, N. Takeda, J Kagami, T. Naoi, Mechanisms of elastic contact and friction between rough surfaces, Wear 48 (1978) 15-34.

24. M. Schoenberg, Elastic wave behavior across linear slip interfaces, Journal of the Acoustical Society of America 68 (1980) 1516-1521.

25. B.W. Drinkwater, R.S. Dwyer-Joyce, P. Cawley, A study of the interaction between ultrasound and a partially contacting solid-solid interface, Proceedings of the Royal Society: Series A 452

(1996) 2613-2628.

26. J. Krautkramer, H. Krautkramer, Ultrasonic Testing of Materials, Springer-Verlag, Fourth Edition, 1990, p.677.

27. T. Arakawa, A study of the transmission and reflection of an ultrasonic beam at machined surfaces pressed against each other, Materials Evaluation 41 (1983) 714-719.

28. K. Hodgson, The Use of Ultrasound to Investigate Engineering, Doctoral Thesis, The University of Sheffield, UK, 2002.

29. M.B. Marshall, R. Lewis, B.W. Drinkwater, R.S. Dwyer-Joyce, An approach for contact stress mapping in joints and concentrated contacts, Journal of Strain Analysis 39 (2004) 339-350.

30. M. Gonzalez-Valadez, R.S. Dwyer-Joyce, Asperity creep measured by the reflection of ultrasound at rough surface contact, ASME Journal of Tribology 131 (2009) DOI:10.1115/1.3089217.

31. I. Yalda-Mooshabad, F.J.Margetan, T.A. Gray, R.B.Thompson, Reflection of ultrasonic waves from imperfect interfaces: A combined boundary element method and independent scattering model approach. Journal of Nondestructive Evaluation 11(3/4) (1992) 141-149.

32. McCool, J.I. Relating profile instrument measurements to the functional performance of rough surfaces, Transactions of the ASME: Journal of Tribology, 109 (1987) 264-270.

33. Nayak, P. Random process model of rough surface, Transactions of the ASME: Journal of Lubrication Technology, 93 (1971) 398-407.

34. I. Sevostianov, M. Kachanov, Normal and tangential compliances of interfase of rough surfaces with contacts of elliptic shape, International Journal of Solids and Structures 45 (2008) 2723-2736.

35. I. Sevostianov, M. Kachanov, Contact of rough surfaces: A simple model for elasticity, conductivity and cross-property connections, Journal of the Mechanics and Physics of Solids 56 (2008) 1380-1400.